Simulating climate with a synchronization-based supermodel

Frank M. Selten,[1, a)] Francine J. Schevenhoven,[2, 3] and Gregory S. Duane[2, 4]
[1)] *Royal Netherlands Meteorological Institute, De Bilt, Netherlands*
[2)] *Geophysical Inst., Univ. of Bergen, Bergen, Norway*
[3)] *Bjerknes Centre for Climate Research, Bergen, Norway*
[4)] *Dept. of Atmospheric and Oceanic Sciences, Univ. of Colorado, Boulder, USA*

(Dated: 22 September 2017)

The SPEEDO global climate model (an atmosphere model coupled to a land and an ocean/sea-ice model with about 250.000 degrees of freedom) is used to investigate the merits of a new multi-model ensemble approach to the climate prediction problem in a perfect model setting. Two imperfect models are generated by perturbing parameters. Connection terms are introduced that synchronize the two models on a common solution, referred to as the supermodel solution. A synchronization-based learning algorithm is applied to the supermodel through the introduction of an update rule for the connection coefficients. Connection coefficients cease updating when synchronization errors between the supermodel and solutions of the "true" equations vanish. These final connection coefficients define the supermodel. Different supermodel solutions, but with equivalent performance, are found depending on the initial values of the connection coefficients during learning. The supermodels have a climatology and a climate response to a CO2 increase in the atmosphere that is closer to the truth as compared to the imperfect models and the standard multi-model ensemble average, showing the potential of the supermodel approach to improve climate predictions.

Keywords: supermodel climate synchronization

Complex numerical codes are being used to predict the behavior of real-world phenomena like the climate or the economy. In this study we demonstrate that predictions can be improved by forming an ensemble of inter-connected different imperfect climate models that synchronize on a common solution, referred to as the supermodel solution. This supermodel solution depends on the connections. The connections are trained using observations of the truth such that the supermodel minimizes synchronization errors when nudged to trajectories of the truth. This is the first time that the potential of the supermodel approach is demonstrated in the context of a complex global climate model. Due to its computational efficiency the synchronization-based learning approach is applicable to state-of-the-art climate models with millions degrees of freedom and historical observations of the Earth's global climate system.

I. INTRODUCTION

Global climate models are complex numerical codes that integrate coupled sets of ordinary differential equations with prescribed time-dependent forcing terms in time in order to produce projections of our future climate. It is commonly found that a multi-model averaged climatology is closer to the observed climatology, which is defined as the average over 30 years and is referred to as the climate normal. Model estimates tend to be distributed around the truth and therefor averaging across models helps in reducing errors in the simulated mean state[20]. Although improved climate statistics are useful, climate adaptation and impact studies often require climate trajectories as input[9]. However averaging trajectories from multiple models without synchronization leads to undesired smoothing and variance reduction.

Here we follow an alternative, synchronization-based approach that produces improved climate trajectories by combining climate models dynamically. This approach was inspired by a study in which two different atmosphere models were coupled to a single ocean model leading to improved climate simulations when the ocean exchanged heat with only one atmosphere model and momentum with the other[12]. Here we dynamically combine models by introducing connection terms into the model equations that nudge the state of one model to the state of every other model in the ensemble, effectively forming a new dynamical system with the values of the connection coefficients as additional parameters. For strong enough connections the models synchronize on a common solution that depends on the values of the connection coefficients[10,13]. This solution is referred to as the supermodel solution[1]. During a learning phase the supermodel is nudged to an observed trajectory and the connection coefficients are adjusted by update rules that depend on the synchronization error. The connection coefficients cease to update when the synchronization is perfect.

So far the supermodel approach was pioneered using relatively simple dynamical systems only[1,5,14] or with very limited inter-model connections in a global climate model context[19]. Here we demonstrate the potential of a fully connected supermodel constructed from versions of

[a)] Author to whom correspondence should be addressed. Email: selten@knmi.nl

a complex global climate model. This model, SPEEDO[18] is described in section II which is followed by a discussion of the supermodel implementation using SPEEDO in section III. The synchronization-based learning is explained in section IV and is applied to the SPEEDO supermodel in section V. In the discussion section VI we discuss the merits of the supermodel approach in relation to the standard multi model ensemble approach. We conclude the paper with a summary of open issues in section VII and discuss the application of the synchronization-based supermodel approach for state-of-the-art weather and climate models.

II. SPEEDO CLIMATE MODEL

The SPEEDO climate model consists of an atmospheric component (SPEEDY) that exchanges information with a land (LBM) and an ocean-sea-ice component (CLIO) using coupling routines (Fig. 1). The coupling routines perform re-gridding operations between the computational grids of the different modules. A detailed description of SPEEDO can be found in[18]. The atmospheric model SPEEDY solves the primitive equations on a sphere using a spectral method[15]. The primitive equations are derived from the Navier-Stokes equations with suitable approximations for atmospheric flow at scales larger than a few kilometers[23]. The spectral expansion into spherical harmonics is truncated at total wavenumber 30 which corresponds to a spatial resolution at the equator of about 700 km. It has 8 vertical levels and relatively simple representations of radiation, convection, clouds, precipitation and turbulent heat, water and momentum exchange at the surface. The solar radiation follows the daily and seasonal cycle. In principle the model consists of 31680 coupled ODE's for the spectral coefficients of the two horizontal wind components U (east-west) and V (north-south), temperature T and specific humidity q at the 8 vertical levels and the log of surface pressure p_s. Calculations in physical space are performed on a Gaussian grid with approximately 3.75 degree spacing (48x96 grid-cells). Speedy exchanges water and heat at the 2115 land points of the land model LBM that uses three soil layers and up to two snow layers to close the hydrological cycle over land and a heat budget equation that controls the land temperatures. The horizontal discretisation is the same as for the atmosphere model. The land surface reflection coefficient for solar radiation is prescribed using a monthly climatology. Each land bucket has a maximum soil water capacity. The runoff is collected in river-basins and drained into the ocean at specific locations of the major river outflows. SPEEDY exchanges heat, water and momentum with the ocean model CLIO[8]. CLIO solves the primitive equations on a computational grid of 3 degree horizontal resolution and 20 unevenly spaced layers in the vertical. It has a rotated grid over the North Atlantic ocean in order to circumvent the singularity at the pole. It has a free-surface and is coupled to a three-layer thermodynamic-dynamic sea-ice model. The sea-ice model takes into account the heat storage in the snow-ice system and calculates the changes of snow and ice thickness in response to surface and bottom heat fluxes. In the computation of ice-dynamics, sea ice is considered to behave as a viscous-plastic continuum as it moves under the action of winds and ocean currents. In total CLIO has about 200.000 degrees of freedom. The SPEEDO equations can be written as

$$\begin{aligned}\dot{\boldsymbol{a}} &= \boldsymbol{f}^a(\boldsymbol{a};\boldsymbol{p}^a) + \boldsymbol{g}^a(\boldsymbol{e}^h,\boldsymbol{e}^w,\boldsymbol{e}^m)\\ \dot{\boldsymbol{o}} &= \boldsymbol{f}^o(\boldsymbol{o};\boldsymbol{p}^o) + \boldsymbol{g}^o(\mathcal{P}^o\boldsymbol{e}^h,\mathcal{P}^o\boldsymbol{e}^w,\mathcal{P}^o\boldsymbol{e}^m,\mathcal{P}^o\boldsymbol{r})\\ \dot{\boldsymbol{l}} &= \boldsymbol{f}^l(\boldsymbol{l};\boldsymbol{p}^l) + \boldsymbol{g}^l(\mathcal{P}^l\boldsymbol{e}^h,\mathcal{P}^l\boldsymbol{e}^w,\boldsymbol{r})\end{aligned} \tag{1}$$

Here we formulate the model in terms of ordinary differential equations (ODEs) on a grid, instead of the more usual partial differential equations (PDEs), to be explicit about the numerical scheme and also for consistency with the ODE scheme for learning intermodel connections that is presented in Section IV. The bold lowercase characters represent vectors with $\boldsymbol{a}$ the atmospheric state vector, $\boldsymbol{o}$ the ocean/sea-ice state vector, $\boldsymbol{l}$ the land state vector, $\boldsymbol{e}^h$ the heat exchange vector between atmosphere and surface, $\boldsymbol{e}^w$ the water exchange vector, $\boldsymbol{e}^m$ the momentum exchange vector and $\boldsymbol{r}$ the river outflows from land to ocean. The exchange vectors depend on the state of the atmosphere and the surface. The projection operators $\mathcal{P}$ represent the re-gridding operations between the computational grids. These operations are conservative so that the globally integrated heat and water loss of the atmosphere at any time at the surface equals the integrated heat and water gain of the land and ocean. The non-linear functions $\boldsymbol{f}$ represent the cumulative contribution of the modelled physical processes to the change in the climate state vector and depend on the values of the parameter vectors $\boldsymbol{p}$. Some of these parameters go through a daily and/or seasonal cycle and/or have a spatial dependence like the reflectivity of the surface. The non-linear functions $\boldsymbol{g}$ describe how the exchange of heat, water and momentum between the subsystems affect the change of the climate state vector.

III. SUPERMODEL

In this study we consider the SPEEDO climate model with standard parameter values as "truth" and create imperfect models of this truth by perturbing parameter values in the atmospheric component. A supermodel is formed by connecting two imperfect atmosphere models through linear nudging terms that nudge the state of model 1 to model 2 and vice versa (see Fig. 2 and (2). Both atmosphere models receive the same state information from the ocean and land model and each calculate their own water, heat and momentum exchange. The ocean and land model receive the exchanges from both atmospheres and use the average of both as input. The supermodel state $\boldsymbol{a}_s$ at any time is defined as the average of both model states. For strong enough nudging both atmospheres synchronize on a common evolution and therefore by taking the averaged state no significant spatial or temporal smoothing is introduced. The SPEEDO super-

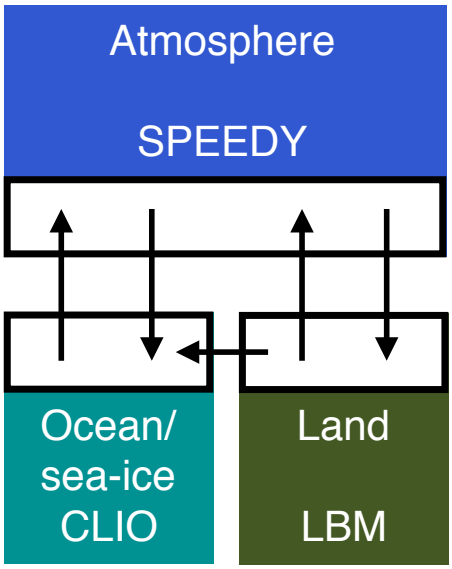

FIG. 1. Schematic representation of the SPEEDO climate model. The atmosphere needs surface characteristics (temperature, roughness, reflectivity) in order to calculate the exchange of heat, water and momentum. Coupler software communicates this information between the components and interpolates between the computational grids.

model equations are given by

$$\begin{aligned}
\dot{\boldsymbol{a}}_1 &= \boldsymbol{f}^a(\boldsymbol{a}_1;\boldsymbol{p}_1^a) + \boldsymbol{g}^a(\boldsymbol{e}_1^h,\boldsymbol{e}_1^w,\boldsymbol{e}_1^m) - \boldsymbol{C}_{12}[\boldsymbol{a}_1-\boldsymbol{a}_2] \\
\dot{\boldsymbol{a}}_2 &= \boldsymbol{f}^a(\boldsymbol{a}_2;\boldsymbol{p}_2^a) + \boldsymbol{g}^a(\boldsymbol{e}_2^h,\boldsymbol{e}_2^w,\boldsymbol{e}_2^m) - \boldsymbol{C}_{21}[\boldsymbol{a}_2-\boldsymbol{a}_1] \\
\dot{\boldsymbol{o}} &= \boldsymbol{f}^o(\boldsymbol{o};\boldsymbol{p}^o) + \boldsymbol{g}^o(\mathcal{P}^o\overline{\boldsymbol{e}^h},\mathcal{P}^o\overline{\boldsymbol{e}^w},\mathcal{P}^o\overline{\boldsymbol{e}^m},\mathcal{P}^o\boldsymbol{r}) \\
\dot{\boldsymbol{l}} &= \boldsymbol{f}^l(\boldsymbol{l};\boldsymbol{p}^l) + \boldsymbol{g}^l(\mathcal{P}^l\overline{\boldsymbol{e}^h},\mathcal{P}^l\overline{\boldsymbol{e}^w},\boldsymbol{r}) \\
\boldsymbol{a}_s &= \frac{1}{2}[\boldsymbol{a}_1+\boldsymbol{a}_2] \qquad (2)
\end{aligned}$$

where $\boldsymbol{C}$ denotes a diagonal matrix with connection coefficients on the diagonal, the subscripts refer to the respective models and the overbar denotes an average over the two models.

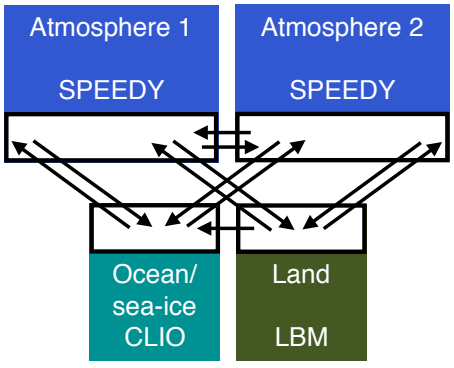

FIG. 2. Schematic representation of the SPEEDO climate supermodel. The two imperfect atmosphere models exchange water, heat and momentum with the perfect ocean and land model. The ocean and land model send their state information to both atmosphere models. The atmosphere models exchange state information with each other.

The supermodel equation can be written as

$$\begin{aligned}
\dot{\boldsymbol{a}}_s =& \frac{1}{2}[\boldsymbol{f}^a(\boldsymbol{a}_1;\boldsymbol{p}_1^a) + \boldsymbol{f}^a(\boldsymbol{a}_2;\boldsymbol{p}_2^a)] + \\
& \frac{1}{2}[\boldsymbol{g}^a(\boldsymbol{e}_1^h,\boldsymbol{e}_1^w,\boldsymbol{e}_1^m) + \boldsymbol{g}^a(\boldsymbol{e}_2^h,\boldsymbol{e}_2^w,\boldsymbol{e}_2^m)] + \\
& \frac{1}{2}[\boldsymbol{C}_{12}-\boldsymbol{C}_{21}][\boldsymbol{a}_2-\boldsymbol{a}_1] \qquad (3)
\end{aligned}$$

From this equation a number of interesting observations can be made. For equal connection coefficients ($\boldsymbol{C}_{12} = \boldsymbol{C}_{21}$) the last term vanishes and the supermodel solution becomes equal to the average of both imperfect model solutions. If the synchronization is perfect ($\boldsymbol{a}_1 = \boldsymbol{a}_2 = \boldsymbol{a}_s$) then the supermodel solution obeys the averaged imperfect model equations with equal weights $\frac{1}{2}$. Solving the weighted averaged equations is referred to as weighted supermodeling[21] as opposed to connected supermodeling. For unequal connection coefficients ($\boldsymbol{C}_{12} \neq \boldsymbol{C}_{21}$), with for instance model 1 more strongly nudged to model 2 than vice versa, the last term is non-zero and systematically pushes the connected supermodel solution every time-step toward the state of model 2 (see Fig. 3).

Negative connection values imply that the model solutions are driven apart. This is undesired as the aim is to synchronize the models on a common solution. Without this constraint, the model with the negative coefficient will be driven away from the other model solution. However, both solutions could still remain close together, if the other model gets a positive connection coefficient with larger value and chases the model with the negative coefficient. In this study we will restrict to positive connection coefficients only.

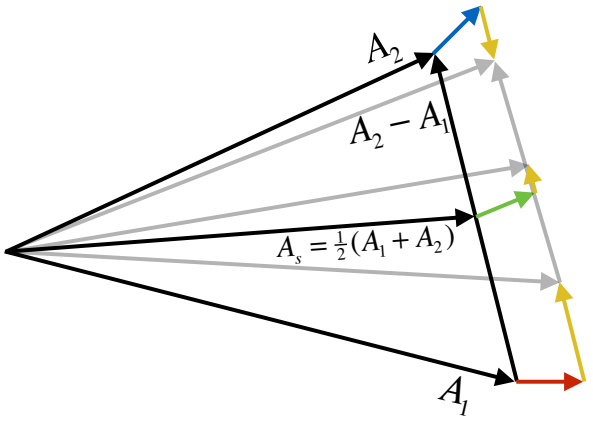

FIG. 3. Graphical representation of one time-step of the connected supermodel. Black arrows denote state vectors at initial time, grey arrows one time-step later. The change in the supermodel state (green vector) is the averaged change of model 1 (red vector) and model 2 (blue vector) plus a vector due to the nudging terms (yellow vectors) pointing in the direction of the model 2 state, assuming that the model 1 state is more strongly pushed to the model 2 state than vice versa.

IV. SYNCHRONIZATION-BASED LEARNING

The supermodel solution (2) depends on the choice of the connection coefficient values $\boldsymbol{C}$. A learning algorithm that extends synchronization of states to synchronization of parameters is applied in order to train the supermodel to follow trajectories from the truth more closely as explained in the next section.

A. From state synchronization to parameter synchronization

Suppose we have two coupled dynamical systems:

$$\begin{aligned}\dot{\boldsymbol{x}} &= \boldsymbol{f}(\boldsymbol{x};\boldsymbol{p})\\ \dot{\boldsymbol{y}} &= \boldsymbol{f}(\boldsymbol{y};\boldsymbol{q}) - \boldsymbol{K}(\boldsymbol{y}-\boldsymbol{x})\end{aligned} \tag{4}$$

where $\boldsymbol{p}$ and $\boldsymbol{q}$ are vectors of parameters, $\boldsymbol{K}(\boldsymbol{y}-\boldsymbol{x})$ is a nudging term that couples the two systems, and $\boldsymbol{K}$ is a diagonal matrix of nudging coefficients. We will assume that the equations are linear in the parameters $\boldsymbol{p}$.

Suppose that when the two systems are identical, i.e. when $\boldsymbol{p} = \boldsymbol{q}$, the two systems synchronize, that is, as $t \to \infty$, $\boldsymbol{y}(t) \to \boldsymbol{x}(t)$. We want to find some rule for varying the parameters $\boldsymbol{q}$, i.e. a dynamical equation such that even if the two systems are not identical, $\boldsymbol{p} \neq \boldsymbol{q}$, the systems will still synchronize, and the parameters will become equal, that is, as $t \to \infty$, $\boldsymbol{y}(t) \to \boldsymbol{x}(t)$, and $\boldsymbol{q}(t) \to \boldsymbol{p}$. The problem is that of "adaptive observers" in the electrical engineering literature[2,24].

First, for concreteness, we show how such a rule might be derived for the simple case of two connected Lorenz systems:

$$\begin{aligned}\dot{x_1} &= \sigma(x_2 - x_1) & \dot{y_1} &= \sigma(y_2 - y_1) - c(y_1 - x_1)\\ \dot{x_2} &= \rho x_1 - x_2 - x_1 x_3 & \dot{y_2} &= \tilde{\rho} y_1 - y_2 - y_1 y_3\\ \dot{x_3} &= -\beta x_3 + x_1 x_2 & \dot{y_3} &= -\beta y_3 + y_1 y_2\end{aligned} \tag{5}$$

where the subscripts refer to the state vector elements.

If $\tilde{\rho} = \rho$, the two dynamical systems are identical and are known to synchonize: As $t \to \infty$, $(y_1(t), y_2(t), y_3(t)) \to (x_1(t), x_2(t), x_3(t))$, and $\boldsymbol{e}(t)^2 \to 0$, where the synchronization error $\boldsymbol{e} \equiv (y_1 - x_1, y_2 - x_2, y_3 - x_3)$. We claim that that in the case of non-identical systems, with $\tilde{\rho} \neq \rho$, we can still arrange for synchronization if we can allow $\tilde{\rho}$ to vary as a new dynamical variable, specifically introducing the dynamical equation for $\tilde{\rho}$:

$$\begin{aligned}\dot{\tilde{\rho}} &= -(y_2 - x_2)y_1\\ &= -e_2 y_1\end{aligned} \tag{6}$$

To see why (6) implies $(y_1, y_2, y_3, \tilde{\rho}) \to (x_1, x_2, x_3, \rho)$, consider the Lyapunov function $L \equiv (y_1 - x_1)^2 + (y_2 - x_2)^2 + (y_3 - x_3)^2 + (\tilde{\rho} - \rho)^2$. If we can show $L(t) \to 0$, we will have the desired state and parameter synchronization. Consider the time derivative

$$\dot{L} = \dot{L}_0 + 2\dot{\tilde{\rho}}(\tilde{\rho} - \rho) \tag{7}$$

where $L_0 \equiv \boldsymbol{e}^2$ is the part of the Lyapunov function formed from state errors alone. The key point is that the time derivative of L_0 differs from its value for $\tilde{\rho} = \rho$, because the dynamical equation for y_2 is different. Specifically, in the derivative

$$\begin{aligned}\dot{L}_0 &= \frac{d}{dt}\left((y_1 - x_1)^2 + (y_2 - x_2)^2 + (y_3 - x_3)^2\right)\\ &= 2(y_1 - x_1)\frac{d}{dt}(y_1 - x_1) + 2(y_2 - x_2)\frac{d}{dt}(y_2 - x_2)\\ &\quad + 2(y_3 - x_3)\frac{d}{dt}(y_3 - x_3)\end{aligned} \tag{8}$$

(where we do not include parameter error explicitly), every term on right hand side is exactly of the same form as in the case of equal parameters, except for the term that contains y_2. The time-derivative factor in that term can be written as:

$$\begin{aligned}\frac{d(y_2 - x_2)}{dt} &= (\tilde{\rho} - \rho)y_1 + \rho y_1 - y_2 - y_1 y_3\\ &\quad - \rho x_1 + x_2 + x_1 x_3\\ &= (\tilde{\rho} - \rho)y_1 + \frac{d(y_2 - x_2)}{dt}|_{\tilde{\rho}=\rho}\end{aligned} \tag{9}$$

where the last term is the value that the time-derivative would have if the parameters were equal. Substituting (9) into (8) gives

$$\begin{aligned}\dot{L}_0 &= 2(y_1 - x_1)\frac{d}{dt}(y_1 - x_1) + 2(y_2 - x_2)\frac{d}{dt}(y_2 - x_2)|_{\tilde{\rho}=\rho}\\ &\quad + 2(y_3 - x_3)\frac{d}{dt}(y_3 - x_3) + 2(y_2 - x_2)(\tilde{\rho} - \rho)y_1\\ &= \dot{L}_0|_{\tilde{\rho}=\rho} + 2(y_2 - x_2)(\tilde{\rho} - \rho)y_1\end{aligned} \tag{10}$$

Inserting (6) and (10) into (7), we have

$$\begin{aligned}\dot{L} =& \dot{L}_0|_{\tilde{\rho}=\rho} + 2(y_2 - x_2)(\tilde{\rho} - \rho)y_1\\ &- 2(y_2 - x_2)(\tilde{\rho} - \rho)y_1\\ =& \dot{L}_0|_{\tilde{\rho}=\rho}\end{aligned} \tag{11}$$

Trajectories of the coupled identical systems monotonically approach synchronization after some point in time, with $\dot{L}_0|_{\tilde{\rho}=\rho} < 0$. So, by (11) the same can be said of the trajectories of the non-identical systems, for which $\dot{L} < 0$. The reason is that the dynamical equation (6) is constructed so that changes in the time-derivative of L due to *explicit inclusion of parameter error in the Lyapunov function* will exactly cancel the changes due to the *implicit effect on the states through the dynamical equations.*

To generalize the above argument to any pair of synchronizing dynamical systems, consider two Lyapunov functions of state error and parameter error:

$$L_0(\boldsymbol{e}) \equiv \boldsymbol{e}^2 = \sum_i e_i^2 \tag{12}$$

$$L(\boldsymbol{e}, \boldsymbol{r}) \equiv \boldsymbol{e}^2 + \boldsymbol{s}^2 = \sum_i e_i^2 + \sum_j s_j^2 \tag{13}$$

where $\boldsymbol{e} = \boldsymbol{y} - \boldsymbol{x}$, and $\boldsymbol{s} = \boldsymbol{q} - \boldsymbol{p}$. Because L_0 and L vanish only when all arguments vanish, if we can show either that $L_0 \to 0$ or that $L \to 0$, we have synchronization. If $L \to 0$, we also have parameter matching.

We seek a dynamical equation for $\boldsymbol{q}$ such that there is a simple relationship between the Lyapunov function for the case of unequal parameters and that for the case of equal parameters. Since we already know $L_0|_{\boldsymbol{p}=\boldsymbol{q}} \to 0$, because the identical systems synchronize, we then have $L \to 0$ as well.

To find a suitable parameter up date rule, $\dot{\boldsymbol{q}} = \boldsymbol{u}(\boldsymbol{x})$, we consider the time derivative of L:

$$\begin{aligned}\dot{L} &= \dot{L}_0 + 2\sum_j s_j \dot{s}_j \\ &= 2\sum_i e_i \dot{e}_i + 2\sum_j (q_j - p_j)\dot{q}_j \end{aligned} \tag{14}$$

recalling that $\dot{p}_i = 0$. We seek to decompose $\dot{e}_i$ in (14) as the sum of the value for a system with $\boldsymbol{q} = \boldsymbol{p}$ and a correction term due to the fact that $\boldsymbol{q} \neq \boldsymbol{p}$:

$$\dot{e}_i = \dot{e}_i|_{\boldsymbol{q}=\boldsymbol{p}} + \sum_j (q_j - p_j)\frac{\partial f_i(\boldsymbol{y};\boldsymbol{p})}{\partial p_j} \tag{15}$$

The partial derivative with respect to parameter p_j is the co-factor of that parameter in the ith dynamical equation, since the parameter only appears linearly. Inserting (15) in (14) yields:

$$\begin{aligned}\dot{L} = \dot{L}_0|_{\boldsymbol{q}=\boldsymbol{p}} &+ 2\sum_i e_i \sum_j (q_j - p_j)\frac{\partial f_i(\boldsymbol{y};\boldsymbol{p})}{\partial p_j} \\ &+ 2\sum_j (q_j - p_j)\dot{q}_j \end{aligned} \tag{16}$$

If we choose a parameter adaptation rule:

$$\dot{q}_j = -\sum_i e_i \frac{\partial f_i(\boldsymbol{y};\boldsymbol{p})}{\partial p_j} \tag{17}$$

then the last two terms in (16) cancel and we have

$$\dot{L} = \dot{L}_0|_{\boldsymbol{q}=\boldsymbol{p}} \tag{18}$$

which we claim is enough to give $L \to 0$, and hence synchronization, in the unequal-parameter case. That is because we already know that the Lyapunov function for the equal-parameter case is monotonically decreasing for some finite region of state space, i.e. $\dot{L}_0|_{\boldsymbol{q}=\boldsymbol{p}} \leq 0$ in this region, and $\dot{L}_0|_{\boldsymbol{q}=\boldsymbol{p}} = 0$ only if $\boldsymbol{x} = \boldsymbol{y}$. Under an assumption of "high-quality synchronization", where after some time there is no bursting away from the synchronization manifold, there is a finite distance from the manifold below which all points belong to the attractive region, so once a trajectory enters the region it cannot leave, since a decreasing L_0 implies decreasing distance from the manifold. Then $\dot{L} \leq 0$ in this region as well, implying $\boldsymbol{y}(t) \to \boldsymbol{x}(t)$, and $\boldsymbol{q}(t) \to \boldsymbol{p}$ as desired. (Strictly speaking, $\dot{L} \leq 0$ could imply that L converges to a positive constant value, and not to 0, but since $\dot{L} = \dot{L}_0|_{\boldsymbol{q}=\boldsymbol{p}} = 0$ only if $\boldsymbol{x} = \boldsymbol{y}$, the strict inequality holds except possibly on the synchronization subspace $\boldsymbol{x} = \boldsymbol{y}$, which is not dynamically invariant except when $\boldsymbol{q} = \boldsymbol{p}$.)

The rule (17) can be generalized a bit: If we start with a more general Lyapunov function $L(\boldsymbol{e}, \boldsymbol{s}) = \boldsymbol{e}^2 + \sum_j \frac{1}{\delta_j} s_j^2$, which is positive definite for arbitrary positive constants δ_j , we can derive a rule:

$$\dot{q}_j = -\delta_j \sum_i e_i \frac{\partial f_i(\boldsymbol{y};\boldsymbol{p})}{\partial p_j} \tag{19}$$

in place of (17). A still more general form of the parameter adaptation rule was proved in[7].

B. Synchronization-based learning of inter-model connections

We apply the parameter adaptation rule (19) to the inter-model connections in a supermodel based on two imperfect SPEEDY atmospheres. The configuration is depicted in Fig. 4 with corresponding equations:

$$\begin{aligned}\dot{\boldsymbol{a}}_0 &= \boldsymbol{f}^a(\boldsymbol{a}_0;\boldsymbol{p}_0^a) + \boldsymbol{g}^a(\boldsymbol{e}_0^h, \boldsymbol{e}_0^w, \boldsymbol{e}_0^m) \\ \dot{\boldsymbol{a}}_1 &= \boldsymbol{f}^a(\boldsymbol{a}_1;\boldsymbol{p}_1^a) + \boldsymbol{g}^a(\boldsymbol{e}_1^h, \boldsymbol{e}_1^w, \boldsymbol{e}_1^m) \\ &\quad - \boldsymbol{C}_{12}[\boldsymbol{a}_1 - \boldsymbol{a}_2] - \boldsymbol{K}[\boldsymbol{a}_1 - \boldsymbol{a}_0] \\ \dot{\boldsymbol{a}}_2 &= \boldsymbol{f}^a(\boldsymbol{a}_2;\boldsymbol{p}_2^a) + \boldsymbol{g}^a(\boldsymbol{e}_2^h, \boldsymbol{e}_2^w, \boldsymbol{e}_2^m) \\ &\quad - \boldsymbol{C}_{21}[\boldsymbol{a}_2 - \boldsymbol{a}_1] - \boldsymbol{K}[\boldsymbol{a}_2 - \boldsymbol{a}_0] \\ \dot{\boldsymbol{o}} &= \boldsymbol{f}^o(\boldsymbol{o};\boldsymbol{p}^o) + \boldsymbol{g}^o(\mathcal{P}^o\boldsymbol{e}_0^h, \mathcal{P}^o\boldsymbol{e}_0^w, \mathcal{P}^o\boldsymbol{e}_0^m, \mathcal{P}^o\boldsymbol{r}) \\ \dot{\boldsymbol{l}} &= \boldsymbol{f}^l(\boldsymbol{l};\boldsymbol{p}^l) + \boldsymbol{g}^l(\mathcal{P}^l\boldsymbol{e}_0^h, \mathcal{P}^l\boldsymbol{e}_0^w, \boldsymbol{r}) \\ \boldsymbol{a}_s &= \frac{1}{2}[\boldsymbol{a}_1 + \boldsymbol{a}_2] \\ \dot{\boldsymbol{C}}_{\mu\nu} &= \boldsymbol{u}_{\mu\nu} \end{aligned} \tag{20}$$

where $\boldsymbol{u}_{\mu\nu}$ denote parameter update rules for the connection coefficient values of model μ nudged to model ν. The two imperfect atmosphere models ($\boldsymbol{a}_1$ and $\boldsymbol{a}_2$) are nudged to the truth ($\boldsymbol{a}_0$) with fixed nudging strength $\boldsymbol{K}$. Truth is represented by the SPEEDY model with standard parameter values ($\boldsymbol{a}_0$). The ocean and land model send their state information to all atmosphere models but receive the water, heat and momentum exchange from the true atmosphere only. The imperfect atmosphere models exchange state information and are nudged to each others state. Note that intermittent nudging of models to reality accomplishes the task of *data assimilation* in numerical weather prediction[6,22], so during training the supermodel effectively does continuous data assimilation.

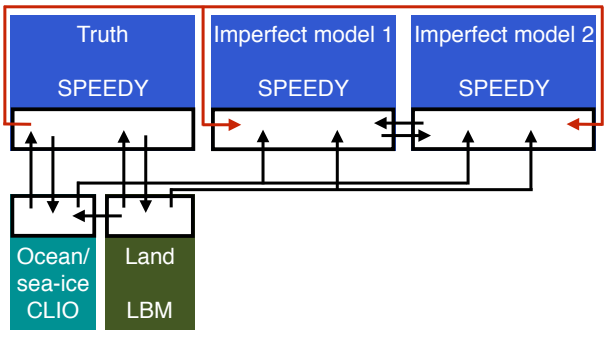

FIG. 4. Schematic representation of the SPEEDO climate supermodel during synchronization-based training.

The parameter adaptation rule for a supermodel is obtained by forming the parameter vector $\boldsymbol{q}$ from the set of connection coefficients $C_{\mu\nu,ii}$, for μ and ν ranging over the labels of the separate models, and the index i over the dimension of the state vector[5]. If one assumes the truth is a supermodel for "correct" values of $\boldsymbol{C}_{\mu\nu}$ then application of the rule (19) to the supermodel (20) using $e_i = a_{s,i} - a_{0,i}$ gives:

$$\dot{C}_{\mu\nu,ii} = \delta_{\mu\nu,i}[a_{\mu,i} - a_{\nu,i}][a_{s,i} - a_{0,i}] \tag{21}$$

where index i is the index of the state vector and the adaptation rates $\delta_{\mu\nu,i}$ are arbitrary constants. In principle the adaptation rates can be chosen different for each inter-model connection element of the state vector, but in this study we will choose a single adaptation rate for all elements and drop the subscripts from here on. The rule (21) has a simple interpretation: the time integral of the right-hand side gives the temporal covariance between truth-supermodel synchronization error, $(a_{s,i} - a_{0,i})$, and the inter-model nudging term, $(a_{\mu,i} - a_{\nu,i})$. It indeed makes sense to adapt the inter-model nudging strength, for a given pair of corresponding variables, depending on the sign and magnitude of this covariance. The connection coefficients cease updating when this covariance is zero and/or the synchronization error vanishes. In principle one could consider allowing different connection strengths for each state vector element. For SPEEDY this would imply adapting $N(N-1)$ times 31680 coefficients with N the number of imperfect models in the supermodel. In this study we will impose spatial invariance on the connection coefficients and only consider dependence on the physical variable that is being nudged in order to keep the number of adjustable coefficients relatively small. The nudging is applied to the velocity and temperature fields only, not to surface pressure and atmospheric humidity. It turns out that synchronization of the total state can be achieved by nudging these three fields only and an advantage is that it requires less communication between the atmospheres during the simulation. This choice for the nudging results in six connection coefficients for the inter-model connections between two imperfect models. The adaptation rules for the connection coefficients become

$$\begin{aligned}
\dot{C}^T_{\mu\nu} = \; & \delta \sum_{k=1}^{8}\sum_{i=1}^{96}\sum_{j=1}^{48}[T_\nu(\lambda_i,\phi_j,p_k) - T_\mu(\lambda_i,\phi_j,p_k)] \\
& \times \; [T_0(\lambda_i,\phi_j,p_k) - T_s(\lambda_i,\phi_j,p_k)] \\
\dot{C}^U_{\mu\nu} = \; & \delta \sum_{k=1}^{8}\sum_{i=1}^{96}\sum_{j=1}^{48}[U_\nu(\lambda_i,\phi_j,p_k) - U_\mu(\lambda_i,\phi_j,p_k)] \\
& \times \; [U_0(\lambda_i,\phi_j,p_k) - U_s(\lambda_i,\phi_j,p_k)] \\
\dot{C}^V_{\mu\nu} = \; & \delta \sum_{k=1}^{8}\sum_{i=1}^{96}\sum_{j=1}^{48}[V_\nu(\lambda_i,\phi_j,p_k) - V_\mu(\lambda_i,\phi_j,p_k)] \\
& \times \; [V_0(\lambda_i,\phi_j,p_k) - V_s(\lambda_i,\phi_j,p_k)]
\end{aligned} \tag{22}$$

where λ_i denotes the longitude, ϕ_j the latitude and p_k the pressure level. The right-hand side of these equations corresponds to the spatial covariance between the truth-supermodel synchronization error and the inter-model nudging terms. The adaptation rule in this case adjusts the connection coefficient of temperature, for example, between model μ and ν when the temperature difference between model μ and ν spatially and temporally covaries with the truth-supermodel synchronization error in temperature. This procedure makes sense because the inter-model temperature difference is proportional to the inter-model nudging term, and one wants to use more or less inter-model nudging, in a given direction, depending on whether the nudging tends to decrease or increase truth-supermodel synchronization error.

V. RESULTS

A. Imperfect models

First SPEEDO with standard parameter values (the "truth") was integrated for 400 years using present-day atmospheric CO_2 concentrations. The global mean surface temperature of this simulation rises from 13 degrees Celsius to about 14.2 degrees during the first 50 years, remains fairly stable for about 300 years and subsequently starts to cool during the final 50 years (Fig. 5). Slow cooling trends in the deep ocean are present during the whole simulation and in the end stabilize the ocean and reduce the mixing of heat from the deep ocean to the cold surface waters in the North Atlantic. Consequently the North Atlantic surface waters cool, Arctic sea-ice expands and the global mean surface temperature drops.

From this simulation we selected January 1, 2001 in the middle of the relatively stable period as initial condition for the supermodel experiments. We integrated SPEEDO for 40 years for two sets of perturbed parameters (Table I). The parameters concern parameterized descriptions of horizontal and vertical mixing processes due to unresolved turbulent motions. Imperfect model 1 (red line) warms around 1.4 degrees with respect to the truth, imperfect model 2 (blue line) cools around 0.5 degrees. The amplitude of these climate differences are not unrealistic as differences of more then a degree in global mean temperature are not uncommon between state-of-the-art climate models. For reference the perfect model was also integrated for 40 years (green line), referred to as the control simulation. It deviates from the truth due to sensitive dependence on initial conditions as it was initiated from a perturbed first of January 2001 state.

	perfect	imperfect 1	imperfect 2
relaxation timescale of convection	6 hours	4 hours	8 hours
relative humidity threshold	0.9	0.85	0.95
momentum diffusion timescale	24 hours	18 hours	30 hours

TABLE I. Parameter values in perfect and imperfect models.

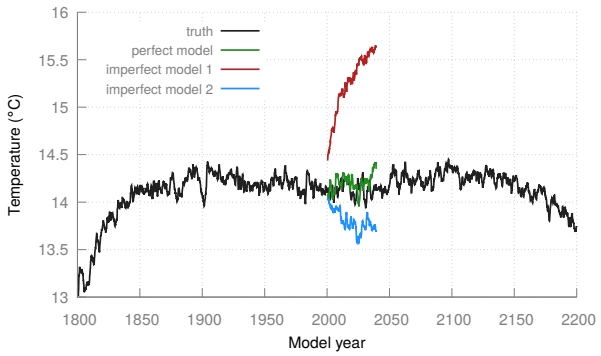

FIG. 5. Global mean temperature time-series for SPEEDO with standard parameter values (truth). The perfect model and the two imperfect models were initiated in year 2001 and integrated for 40 years.

B. Synchronization

Before we start to connect the two imperfect models and train the connection coefficients, we first have a look at the synchronization errors when the models are nudged to the truth.

During training synchronization errors determine the updates to the connection coefficients. For effective training synchronization errors should be significantly larger for the imperfect models than for the perfect model for given model-to-truth nudging strength $\boldsymbol{K}$. Ideally the trained supermodel will have synchronization errors close to the perfect model. We investigated the magnitude of the synchronization error in relation to the nudging strength $\boldsymbol{K}$ by running the configuration depicted in Fig. 6. The perfect and imperfect models receive the state information from the truth at every time-step and their states are nudged accordingly. Only the truth exchanges water, heat and momentum with the surface (ocean and land) models. The other models receive the state information from the surface models, calculate each their own water, heat and momentum exchange, but this information is not communicated back to the surface models.

The models are initialized from randomly perturbed January 1, 2001 states and integrated for two weeks with $\boldsymbol{K}$ set to zero in order to allow the models to desynchronize. Next $\boldsymbol{K}$ is set to a value of $1/24$ hours^{-1} and the integration is continued for the rest of the year. Sensitive dependence on initial conditions and model errors cause a rapid increase of the synchronization error during the first two weeks (Fig. 7a). The error reduces rapidly when $\boldsymbol{K}$ is set to $1/24$ hours^{-1} after two weeks, levels off within a couple of weeks and remains fairly stable for the remainder of the year. The perfect model does not synchronize perfectly with the truth, but the average error is only 0.01 degree Celsius. Given daily fluctuations at given locations of tens of degrees, this is a very small synchronization error. The synchronization error is about 10 times larger for imperfect model 1 and 6 times for imperfect model 2. The synchronization error is almost independent of nudging timescale between 24 and 4 hours for the perfect model, but for the imperfect models the errors are reduced by more than 60 % over this range (Fig. 7b). Note that nudging only part of the total state vector (the surface pressure field and the humidity field are not nudged) is sufficient to achieve this high degree of synchronization.

Based on these synchronization experiments we choose a nudging timescale of 24 hours. The nudging keeps the imperfect models close to the truth, but at the same time there is room for a ten-fold reduction in synchronization error by updating the inter-model connection coefficients.

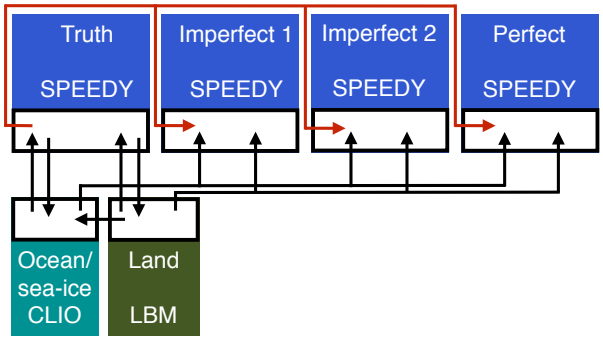

FIG. 6. Schematic representation of the SPEEDO configuration for the synchronization experiments.

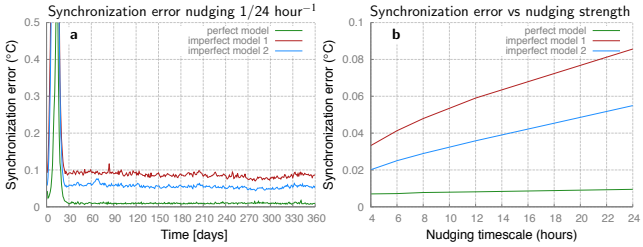

FIG. 7. (a) Synchronization error as measured by the root of the globally averaged mean squared surface air temperature difference between model and truth for a nudging timescale of 24 hours for the perfect model (green), imperfect model 1 (red) and imperfect model 2 (blue). (b) Time-averaged synchronization error during the final 10 months of the integrations as a function of nudging timescale.

C. Learning

In the first learning experiment, the SPEEDO supermodel was initialized at January 1, 2001 in the configuration depicted in Fig. 4 using initial connection coefficient values in (22) equal to $1/8$ hours^{-1}. The nudging timescale corresponding to $\boldsymbol{K}$ in (20) was set to 24 hours as motivated in the previous section. The rate of learning δ in the update rules of (22) was set to 24000. With these parameter choices the SPEEDO supermodel was trained for 10 years by integrating (20) with update rules $\boldsymbol{u}_{\mu\nu}$ given by (22). The six connection coefficients ($C^T_{\mu\nu}$, $C^U_{\mu\nu}$, $C^V_{\mu\nu}$ in Fig. 8ab) converge within the first months to values that remain fairly stable during the remaining 10

years of the training. A small annual cycle is visible suggesting that the optimal nudging coefficients have a weak seasonal dependence. It is obvious from the graph that C_{12} and C_{21} lie symmetrical around the initial value for each of the three variables. This is due to the fact that according to the update rules (22) $\dot{C}_{\mu\nu} = -\dot{C}_{\nu\mu}$. Another consequence is that the asymptotic values depend on the initial value.

In the second learning experiment, the SPEEDO supermodel was initialized with connection strengths equal to 1/24 hours^{-1}. Indeed the asymptotic values are different in this case (Fig. 8cd). In addition the symmetry is broken due to additional constraints that the connection values are not allowed to go below zero or above 1/4 hours^{-1}. An upper bound is imposed in order to prevent numerical instabilities for too strong nudging and allow some desynchronization at times when the truth is hard to follow by both imperfect models. The numerical instabilities could be prevented by reducing the time-step but we chose to keep the time-step fixed at 30 minutes and impose an upper bound on the nudging strength.

The learning experiments result in different supermodel solutions as defined by the asymptotic connection values. These are summarized in Table II. The synchronization error when connected to the truth is similar for both supermodels (Fig. 9), despite the difference in the connection values. The connections of supermodel 1 are about twice as strong as the connections of supermodel 2. The relative strengths between the connections are therefor about the same. This suggests that only the relative strengths matter and that the supermodel solution is invariant under multiplication of all connections by a constant factor provided that the imperfect models synchronize. The initial value of the coefficients during learning selects a particular factor.

It appears that short training periods suffice to train the inter-model connection coefficients, despite the long time-scales present in the climate. During the learning phase the imperfect atmosphere models receive the true ocean, land and sea-ice states and are able to learn how the true atmosphere interacts with these states. The imperfections concern fast atmospheric processes (turbulence and convection) and can thus be trained on these time scales. In order to verify that the training of the inter-model connection coefficients does not depend on the ocean/sea-ice state, we repeated the learning experiments starting in year 2151 of the reference simulation. The state of the ocean and sea-ice is different and the thermo-haline circulation in the North-Atlantic basin is about to collapse, causing a rapid cooling of the sea surface temperatures in the North-Atlantic and a growth of the Arctic sea-ice cover. Nevertheless, the training converges on similar connection values (not shown).

The trained supermodels have smaller synchronization errors as compared to both imperfect models (Fig. 9) but not as small as the perfect model. For comparison we evaluated the synchronization errors of the untrained supermodel with equal weights of 1/24 hours^{-1}. The training has reduced the synchronization error in the east-west component of the wind at 850 hPa by only a small margin (Fig. 9).

It is hoped that the reduction in synchronization error when the supermodel is nudged to truth will be reflected in improved simulations of climate when the supermodel is run freely to simulate climate. If indeed only the relative strengths of the connections matter, then both supermodel solutions should give similar results. In the next sections we will investigate climate simulations of both supermodel solutions in comparison to the perfect and imperfect models and the untrained supermodel.

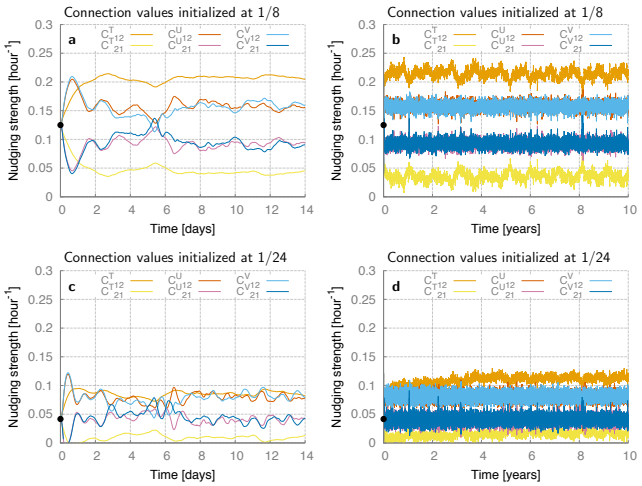

FIG. 8. Time-series of the connection coefficients during the training when initialized at 1/8 hours^{-1} (a and b) and 1/24 hours^{-1} (c and d). The first 14 days of the training are plotted in the left panels, right panels display the whole 10 year training period. The black dot denotes the initial values.

	C_{12}^T	C_{21}^T	C_{12}^U	C_{21}^U	C_{12}^V	C_{21}^V
supermodel 1	0.22	0.03	0.17	0.08	0.17	0.08
supermodel 2	0.12	0.01	0.08	0.04	0.08	0.04

TABLE II. Connection coefficient values of the two supermodel solutions.

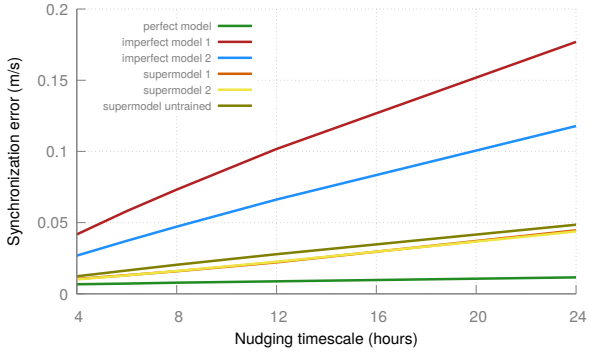

FIG. 9. The globally averaged synchronization error in the east-west component of the wind at 850 hPa for different models when connected to the truth for different nudging strengths from similar synchronization experiments as in Fig. 7b.

D. Climate

The two trained supermodels and the untrained supermodel are initialized at January 1, 2001 and integrated for 40 years. The evolution of the global mean temperature of both trained supermodels shows no sign of a drift with respect to the truth or the perfect model, unlike the imperfect models and the untrained supermodel (Fig. 10). The synchronized evolution of the imperfect models in the untrained supermodel produces a global mean temperature close to the average of the global mean temperature of the two imperfect model evolutions.

In the trained supermodels imperfect model 1 is more strongly nudged to imperfect model 2 for all connections than vice versa (Table II). In this case (3) implies that the supermodel solution is systematically pushed away from the averaged solution toward the evolution of imperfect model 2. This makes sense as the warming of imperfect model 1 with respect to the truth is stronger than the cooling of imperfect model 2 (Fig. 10).

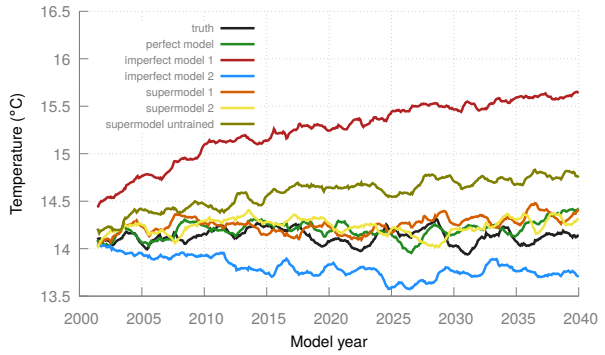

FIG. 10. The global mean surface temperature evolution for the truth, the perfect model, the two imperfect models, the two trained supermodels and the untrained supermodel. All models are initialised at January 1, 2001 of the truth.

Another measure of the quality of the climate simulations are errors in the climatological mean fields. As an example Fig. 11 shows the error in the time average over the final 30 years of the simulations of the east-west component of the wind at the 200 hPa pressure level (at about 10 km height). The mean winds of imperfect model 1 have errors that reach 5 m/s in the Southern Hemisphere. The error pattern has a rich spatial structure, but is to a considerable extent opposite in sign as compared to imperfect model 2. An improved estimate of the true mean winds is obtained by taking the average of both models, commonly referred to as the multi-model average in climate science. The error pattern of the multi-model average is very similar to the error pattern of the untrained supermodel with equal coefficients. Both trained supermodels have smaller errors than the untrained supermodel. The training based on synchronization errors, essentially a training based on short-term prediction errors, has also proved useful for supermodel simulation of long-term climate. For reference the bottom panel of Fig. 11 shows the errors of the perfect model. Due to sampling uncertainties the mean state of the truth is not exactly reproduced in a 30 year simulation with the perfect model. The errors in the mean state of the trained supermodels are larger as compared to the perfect model, especially in the tropical region. An optimally weighted multi-model average was determined and is also shown in Fig. 11. Adding 0.24 times the mean state of imperfect model 1 and 0.76 times the mean state of imperfect model 2 leads to a similar estimate of the true mean state as provided by both trained supermodels.

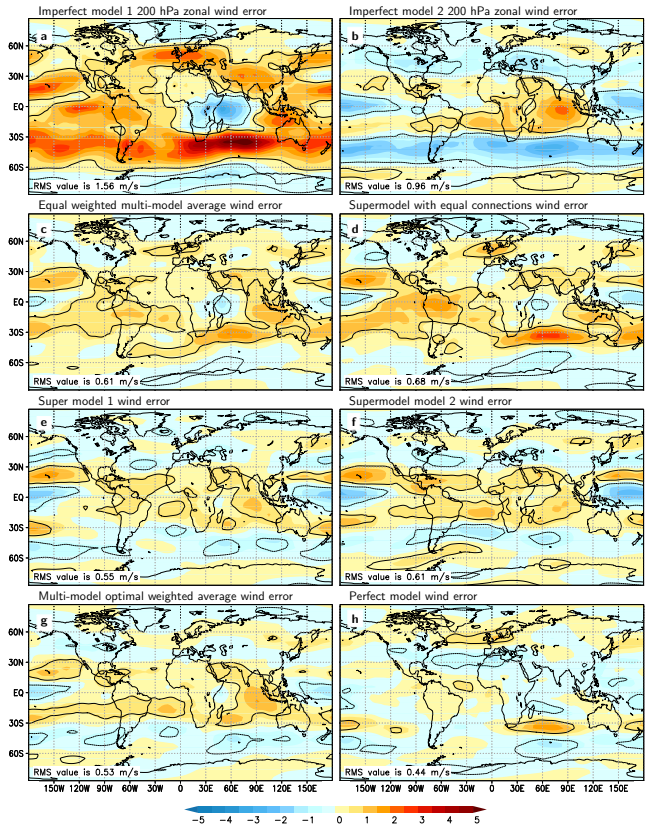

FIG. 11. Difference in the east-west component of the wind at the 200 hPa pressure level averaged over model years 2011-2040 for the various models with respect to the truth. Contours denote areas where the difference is larger than the sampling error at 95% confidence (solid for positive difference, dotted for negative). Positive values imply stronger mean winds blowing eastward. Units: m/s.

Globally averaged errors for a number of different climatological fields paint the same picture (Fig. 12). The untrained supermodel has similar errors as the multi-model average. An optimally weighted multi-model average has smaller errors, comparable to those of the trained supermodels, in the nudged variables and also in variables that are not nudged, like precipitation and cloud-cover. There is still room for some improvement to match the small errors (due to sampling) obtained with the perfect model simulation.

Ideally one should compare attractors in order to make judgements about the quality of the climate simulations instead of just comparing the mean states. For such high-dimensional systems as SPEEDO the evaluation of the probability density in state space is computationally too

expensive since too much data is required in order to yield representative results[3], but other statistical properties of the attractors might be compared. As an example we evaluated the 95% percentile of three-hourly sums of convective rainfall at each location. The results are plotted in Fig. 13. The convective rainfall extremes are largest in tropical areas and in the regions of the extra-tropical stormtracks (panel a). In general imperfect model 1 overestimates and imperfect model 2 underestimates the convective precipitation extremes (panel c and d). Supermodel 1 simulates the precipitation extremes more accurately. The root mean squared error is 1.2 mm/day as compared to 2.7 and 2 mm/day for imperfect model 1 and 2 respectively.

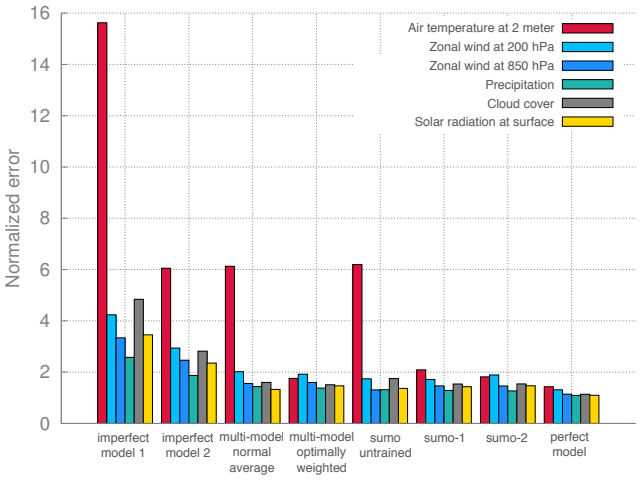

FIG. 12. Normalized errors with respect to the truth in various meteorological fields averaged over model years 2011-2040 for the various models. At each location the difference in the mean state is normalized by 1.96 times the standard deviation of the 30 yearly values, divided by square root of 30. The normalized errors in this graph correspond to the root of the globally averaged squared normalized differences. With this normalization the perfect model has errors around value one.

E. Climate response

Climate models are commonly used to make projections of the future climate by assuming scenarios for future emissions of greenhouse gasses. Here we explore whether the trained supermodel is capable of simulating the climate change due to a doubling of the CO_2 concentration. In model year 2041 the CO_2 concentration is doubled and the various models are integrated for 30 years. Global mean temperature time-series are plotted in Fig. 14. The global mean temperature in the supermodel remains close to the truth after the doubling of CO_2. Imperfect model 1 and 2 simulate a similar warming but the reference state at the onset of doubling is warmer in imperfect model 1 and colder in imperfect model 2. In response to the CO_2 change, also the atmospheric circulation changes (Fig. 15). The change of the east-west component of the wind at 850 hPa in the

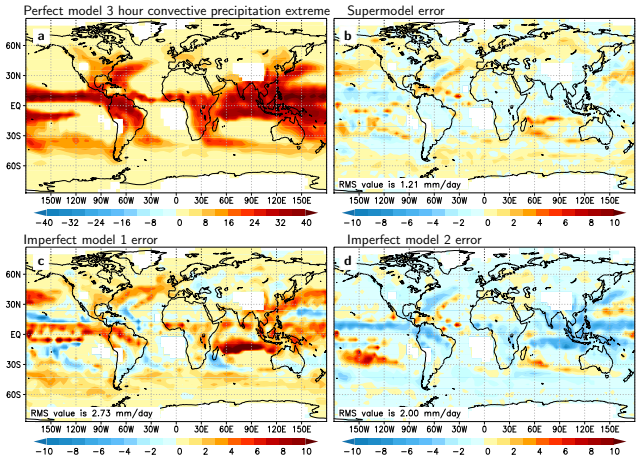

FIG. 13. 95% percentile of convective precipitation three-hourly sums (mm/day) in the perfect model (a), and differences with respect to the perfect model for supermodel 1 (b) and both imperfect models (c and d). Calculations are performed for the years 2011-2040.

supermodel is best simulated by the supermodel (15), especially in the tropical regions around Indonesia.

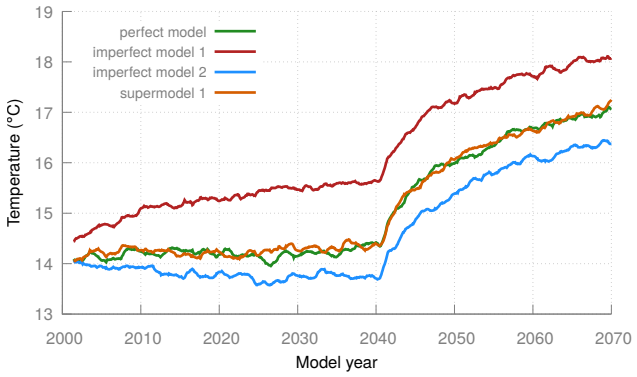

FIG. 14. Global mean temperature time-series for the various models. In model year 2041 the CO_2 concentration is doubled and in response the climate starts to warm.

VI. DISCUSSION: SUPERMODELING VERSUS *A POSTERIORI* COMBINATIONS OF MODEL RESULTS

When compared to the optimally weighted multi-model mean, the supermodel yields similar accuracy. However, in addition the supermodel produces actual trajectories that are closer to the true trajectories. Temperature time-series of imperfect model 1 are systematically too warm in most geographical locations and too cold in imperfect model 2. These time-series cannot be averaged to more accurately represent true time series since the time-series are not synchronized and their mean is not a solution of the dynamical equations. In the supermodel the models converge on a synchronized time-series with a more accurate mean temperature. For climate impact

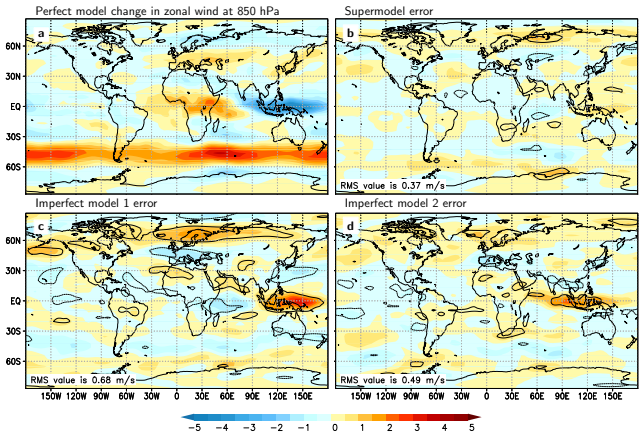

FIG. 15. Change in the east-west component of thef wind at 850 hPa due to a CO_2 doubling in the perfect model (a) and the error in the simulated wind change for supermodel 1 (b) and both imperfect models (c and d). The change is calculated by subtracting the average wind before CO_2 doubling during model years 2016-2040 from the average wind during 2056-2070. The contours indicate regions where the difference is statistically significant at the 95% confidence level. The root of the global mean squared error is plotted in the lower left corner.

studies this is a great advantage since it eliminates the need for bias corrections (correction of time-series in order to remove the error in the mean).

One is interested not only in the mean behavior of the models and supermodel, but in internal variability. The interesting properties of the various attractors are usually captured in probability density functions (pdf's). There is significant ambiguity in methods to combine pdf's of different climate models. Suppose, as a thought experiment, that one has two different models of the same system, each of which exhibits Gaussian statistics in some variable, but with different means and different variances. That is, suppose that the pdf of some state variable x is given by pdf's P_1, P_2 in the two models:

$$P_1(x) = N_1 \exp \frac{(x-\mu_1)^2}{2\sigma_1^2}$$
$$P_2(x) = N_2 \exp \frac{(x-\mu_2)^2}{2\sigma_2^2} \qquad (23)$$

where $N_{1,2}$ are normalization factors. If the means are not greatly separated $|\mu_1 - \mu_2| < \sigma_1, \sigma_2$ and the shapes are similar, $\sigma_1 \approx \sigma_2$, we might guess that the difference is due to some systematic error and that the true distribution is a Gaussian with the average mean:

$$P_m(x) = N_m \exp \frac{(x-\mu_m)^2}{2\sigma^2} \qquad (24)$$

with $\mu_m = (\mu_1 + \mu_2)/2$, and $\sigma \approx \sigma_1 \approx \sigma_2$. If we were instead to blindly average the pdfs, we would in general have a non-gaussian distribution with $\sigma > \sigma_1, \sigma_2$, incorrectly inflating the variance. So it might seem that a recipe for intelligently combining pdfs is accessible.

But what if the true distribution were bimodal, with the means of the two modes more widely separated than in the above case of small systematic error, and what if each model, for reasons of its own dynamical imperfections, is biased in favor of one mode? Then a simple average of pdf's, that would capture the bimodality, would be preferable to the "intelligent" combination described. Without prior information about the form of the true distribution, no general prescription for combining the pdf's is possible. It might not even be possible at all to combine the pdf's of different models into a pdf that reflects the true model well. In[1] for example, two periodic attractors and one stable fixed point attractor were used to construct a chaotic supermodel. The supermodel has similar statistics compared to the true chaotic system, while a combination of the pdf's of the non-chaotic systems cannot give a good approximation of the true chaotic pdf. The extent to which such extreme behavior occurs in real climate models is an open question, but the construction of an actual dynamical system is arguably the soundest way to represent the true physical variations within the modeled climate.

The choice of models in a supermodel configuration is also more flexible than in multi-model averaging. In cases where the constituent models are all on one side of the truth, the introduction of an additional imperfect model into the supermodel that is on the opposite side can help to improve the supermodel[16]. But unlike the situation with multi-model averaging, the new imperfect model, included in the scheme with significant weight, can be a highly unrealistic model, such as one with a fixed-point attractor.

Finally, it should be mentioned that there is one advantage of multi-model runs that naively appears to be lost in supermodeling: the ability to extract spread information from an ensemble of models, as an indicator of model error. But one can easily consider an ensemble of supermodels[4], defined by variations in the connection coefficients determined from fluctuations during the learning process or from different learning strategies. The ensemble spread enables to gauge uncertainties due to model errors and due to imperfect knowledge of the initial state.

VII. SUMMARY AND CONCLUDING REMARKS

This is the first time that synchronization-based supermodeling is applied to complex global climate models and its potential to improve climate simulations is demonstrated. The SPEEDO climate model with standard parameter values is regarded as truth, two imperfect models are constructed by perturbing three parameters. Due to the different parameter setting, one model warms with respect to the truth, the other cools. A supermodel is constructed by connecting the temperature and velocity fields of both models through nudging terms and the supermodel synchronizes on a common solution. Imposing spatial invariance while allowing different connection strengths for the different meteorological fields yields six adjustable connection coefficients. Using the fact that synchronization of states between two connected systems can be extended to synchronization of

parameters, when these vary between the two systems, the inter-model connection coefficients within the supermodel are dynamically adjusted, along with the states, so that the supermodel synchronizes with truth, from which it continuously receives data in the learning phase. After a quick adjustment during the first couple of weeks of the training, the coefficients exhibit only small fluctuations around a stable long-term mean value during the ten year training period. These stable, long-term mean values of the coefficients define the supermodel. During a 40 year climate simulation the supermodel preserves the correct global mean temperature. Moreover the globally averaged errors in all 30 year mean meteorological fields examined are smaller than the errors in the imperfect models. In addition the supermodel is able to reproduce the correct warming in response to a doubling of the CO_2 concentration.

The synchronization-based learning algorithm reaches locally optimal values of the connection coefficients. There appears to be a degeneracy, as explained in Section V C in that, depending on initial coefficient values, the algorithm picks from a family of equally good coefficient values - we conjecture that what matters is not the absolute value of the connection coefficients, but their relative strengths. On the other hand, a more refined connection scheme might yield even better results. During learning the connection values exhibit a weak dependence on the seasonal cycle, for instance, suggesting that a seasonal dependence of the connection strengths might further improve the supermodel climate simulations.

There is no guarantee that the learning algorithm converges on the globally optimal connection coefficients. Other learning approaches based on matching finite segments of the trajectories instead of just the instantaneous states, as in[1], or minimization of errors in climate statistics like the mean or the variance over multi-year long trajectories by iterative methods as in[17,21], might yield even better supermodel solutions.

In state-of-the-art weather forecasts, models are initialised from observed states that are not on the model attractor. During the forecasts the trajectories systematically transition to the model attractor and in a couple of weeks most of the long-term climate errors have developed[11]. We therefor expect that the training based on short-term prediction errors in this study could also be successfully applied to state-of-the-art weather and climate models. We restricted the evaluation of the supermodel to climate timescales, but we expect that short-term prediction errors are improved with respect to the imperfect models since the learning is based on one time step predictions of the truth. Weather prediction with supermodels remains to be evaluated.

In the present study only imperfections in the atmospheric component have been considered. It remains to be seen how imperfections in the land- and ocean models affect the learning. In principle the supermodel approach can be extended to include multiple imperfect ocean- and land models with inter-model connections that can be included in the learning.

The magnitude of the synchronization errors between supermodel and truth is only slightly reduced when the learning process is initialized with uniform connections. Nevertheless, the climate properties of the supermodel with the learned coefficients are much better than those of the supermodel with the initial connection coefficients. It seems that even a small reduction of synchronization error in the training phase is heuristically useful for correcting the dynamics of the model, but more work is needed to assess the universality of this behavior.

Nonnegative connection coefficients are imposed during the learning in order to induce synchronization of the imperfect models in the supermodel. One could allow negative coefficients during the learning. In that case one model tries to flee from the other model, but at the same time the other model chases that model at a faster pace and the imperfect model trajectories can still remain approximately in synch. Other regions of phase space can be explored by the supermodel by allowing negative connections, which might lead to an improved supermodel solution.

Although the supermodel is not trained to be able to simulate the correct response of the climate to a perturbation like the doubling of the atmospheric CO_2 concentration, we find this to be the case in this study. The full extent of the robustness of the supermodel solution against variations in ancillary parameters remains to be determined.

In the perfect model approach of the present study, the truth is inside the model class of imperfect models. It remains to be seen how well the supermodel scores when the truth is outside of the imperfect model class, a situation that arises when climate models are used to simulate a much more complex reality[21].

In applying the supermodel approach to an ensemble of different, state-of-the-art climate models, it must be noted that the different models employ different numerical representations of the various meteorological fields, and especially that they are formulated on different numerical grids. SPEEDO models have been shown to synchronize even when only some meteorological fields are connected, or only some spatial scales. One solution to the problem of different numerical grids would be to transform the grid representation to a spectral representation and do the exchange of state information and nudging in spectral space only for wavenumbers that are well resolved in all participating models in the supermodel, and then transform the nudging tendencies back to the respective grids. Synchronization of the constituent models might be expected, despite the different grid representations.

In the present study we have assumed perfect knowledge of the truth. In reality observations of the truth are incomplete and noisy. The influence of noisy and incomplete observations on the learning of the supermodel remains to be investigated, but we are encouraged by the success of data assimilation for weather prediction under the same circumstances.

We have applied the supermodel approach in the context of simulating the Earths climate, but its application domain is much wider. In any modeling context where different models exist of a complex, real system, like ecological systems or economical systems, where data assimilation from the real systems yields truth-model synchronization, and where enough good

quality observational data is present, the supermodel approach potentially leads to more accurate predictions.

ACKNOWLEDGMENTS

We wish to acknowledge the support of Camiel Severijns and Paul Hiemstra in coding the SPEEDO supermodel. This work is partly funded by STERCP (ERC project 648982)

[1]van den Berge, L. A., Selten, F. M., Wiegerinck, W., and Duane, G. S., Earth System Dynamics **2**, 161 (2011).
[2]Besançon, G., León-Morales, J. D., and Huerta-Guevara, O., International Journal of Control **79**, 581 (2006).
[3]Dool, H. V. D., Tellus A **46** (2011).
[4]Duane, G., Wiegerinck, W., Selten, F., Shen, M.-L., and Keenlyside, N., Chapter in Advances in Nonlinear Geosciences, ed: A.A. Tsonis (2017), 10.1007/978-3-319-58895-7.
[5]Duane, G. S., Entropy **17**, 1701 (2015).
[6]Duane, G. S., Tribbia, J. J., and Weiss, J. B., Nonlinear Processes in Geophysics **13**, 601 (2006).
[7]Duane, G. S., Yu, D., and Kocarev, L., Physics Letters A **371**, 416 (2007).
[8]Goosse, H. and Fichefet, T., Journal of Geophysical Research: Oceans **104**, 23337 (1999).
[9]Hazeleger, W., van den Hurk, B. J. J. M., Min, E., van Oldenborgh, G. J., Petersen, A. C., Stainforth, D. A., Vasileiadou, E., and Smith, L. A., Nature Climate Change **5**, 107 (2015).
[10]Hiemstra, P. H., Fujiwara, N., Selten, F. M., and Kurths, J., Nonlinear Processes in Geophysics **19**, 611 (2012).
[11]Jung, T., Miller, M. J., Palmer, T. N., Towers, P., Wedi, N., Achuthavarier, D., Adams, J. M., Altshuler, E. L., Cash, B. A., III, J. L. K., Marx, L., Stan, C., and Hodges, K. I., Journal of Climate **25**, 3155 (2012).
[12]Kirtman, B. P., Min, D., Schopf, P. S., and Schneider, E. K., Unpublished report , 48 pp (2003).
[13]Lunkeit, F., Chaos: An Interdisciplinary Journal of Nonlinear Science **11**, 47 (2001).
[14]Mirchev, M., Duane, G. S., Tang, W. K., and Kocarev, L., Communications in Nonlinear Science and Numerical Simulation **17**, 2741 (2012).
[15]Molteni, F., Climate Dynamics **20**, 175 (2003).
[16]Schevenhoven, F. J. and Selten, F. M., Earth System Dynamics **8**, 429 (2017).
[17]Severijns, C. A. and Hazeleger, W., Journal of Climate **18**, 3527 (2005).
[18]Severijns, C. A. and Hazeleger, W., Geoscientific Model Development **3**, 105 (2010).
[19]Shen, M.-L., Keenlyside, N., Selten, F., Wiegerinck, W., and Duane, G. S., Geophysical Research Letters **43**, 359 (2016).
[20]Weigel, A. P., Liniger, M. A., and Appenzeller, C., Quarterly Journal of the Royal Meteorological Society **134**, 241 (2008).
[21]Wiegerinck, W. and Selten, F., Chaos **ibid** (2017).
[22]Yang, S., Baker, D., Li, H., Cordes, K., Huff, M., Nagpal, G., Okereke, E., Villafae, J., Kalnay, E., and Duane, G., Journal of the Atmospheric Sciences **63**, 2340 (2006).
[23]Zdunkowski, W. and Bott, A., *Dynamics of the Atmosphere: A Course in Theoretical Meteorology* (Cambridge University Press, 2003).
[24]Zhang, Q., IEEE Transactions on Automatic Control **47**, 525 (2002).